EVOLUTION EQUATIONS BASED APPROACH FOR MODELING FATIGUE IN AMORPHOUS GLASSY POLYMERS. ON THE INVESTIGATION OF FATIGUE DAMAGE DEVELOPMENT IN POLYCARBONATE

Sami Holopainen[1]

[1]Tampere University of Technology, Department of Mechanical Engineering and Industrial Systems
P.O. Box 589, FI-33101 Tampere, Finland
e-mail: sami.holopainen@tut.fi

Keywords: fatigue, damage, amorphous glassy polymers, endurance surface.

Abstract. *While the key damage processes for focusing on the macroscopic mechanical behavior of amorphous glassy polymers are already well identified, relevant deformation mechanisms for fatigue damage are not yet established. The underlying study was born from the wish to gain some better understanding of how said mechanisms contribute to the fatigue damage in amorphous glassy matrix. In order to investigate the issue, an approach suitable for modeling fatigue in amorphous glassy polymers is proposed. The approach is calibrated to data taken from isothermal fatigue tests on dumbbell shaped PC-specimens. To investigate fatigue versus inhomogeneous deformation behavior, the approach is implemented in a finite-element program.*

1 INTRODUCTION

Manufacturers of polymer materials are being interested in assurance of components' lifetime, especially when the lifetime cannot be easily inspected or may lead to a catastrophe in service, [30]. Examples of mechanical components that are manufactured from polymers and may experience fatigue during their service life are found e.g. from medical industry, automotive glazing, aeronautics, and armour, [37], [24]. The design of such constructions could benefit from capable models and the strong computational capability available nowadays.

The knowledge of the ultimate behavior of amorphous glassy polymers has been developed rapidly while only a little of this work has been devoted to fatigue. Specific features of fatigue failure development are found e.g. from [40], [3], and [31]. To explore materials' microstructural characteristics with regard to fracture toughness, a strong attention has been paid on the damage mechanisms ahead of the crack tip, cf. [39], [36], [7], and [16] to mention a few. Much research has also devoted to the investigation of fatigue crack propagation in polymer composites having strong directional mechanical properties, cf. e.g. [12], [20], [19]. However, those fracture mechanics approaches neglect the crack initiation stage which may cover over 90% of the total fatigue life of amorphous polymers, [18].

Fatigue failure of amorphous polymers in their glassy state (termed amorphous glassy polymers) is generally due to a two-step process. In the first, initiation step failure is typically attributed to deficiencies or impurities affecting significant stress concentrations which exceed the strength limits of the material, [12], [23]. Under repeated loadings, those defects can nucleate and grow during the service life even at stress levels well below the nominal yield strength, [7], [27]. This part of fatigue is influenced by the localized yield-like deformation process which provides fatigue crack initiation sites controlling fatigue life (number of cycles N to failure) and thus being of a specific interest in the applied fatigue stress S (S-N curve), [23], [22]. The second, propagation step is characterized by the growth of damage through the coalescence of micro-cracks and propagation of small cracks to form large cracks which ultimately cause component failure, [21], [22]. However, the duration of the initiation step is typically orders of magnitude greater than the propagation time and thus plays most important role on fatigue behavior, [18]. Based on this observation the influence of crack propagation in the material behavior is often omitted in the fatigue models.

Fatigue failure of polymers is generally due to either mechanically or thermally dominated mechanisms. Mechanical modes that occur relatively low stresses and frequencies are characterized by the two step process described above. The macroscopic mechanical behaviour under such conditions is primarily (visco)elastic being influenced by the defects or inhomogeneities in material, [3], [17]. The fatigue life is relatively long while the ultimate fracture mechanism is rather brittle and influenced by combined mechanisms of the plastic dilatation and coalescence of inclusions or voids, [23], [28]. In thermally dominated mechanisms, at relatively high stresses and frequencies, the physical and mechanical properties of the polymer change due to hysteretic heating. This characteristic results from a high internal damping and low thermal conductivity of polymers when heat generated from mechanical fatigue cannot be dissipated to the surroundings, [41], [40], [18]. The time to thermally dominated failure is often rather short and the failure mode ductile, [4], [3], [17].

From a mesoscopic point of view, shear yielding and crazing, subsequent crack initiation and propagation are assumed to be major mechanisms for fatigue development in amorphous polymers. However, through existing literature of the field, key morphological or microstructural mechanisms that could explain their origin and subsequent progress of fatigue damage both in

homogenous and in toughened amorphous polymers are unclear at this moment.

The article continues by introducing a novel model suitable for predicting fatigue in amorphous glassy polymers. The governing constitutive model employed is an extension of the celebrated Boyce-Park-Argon (BPA) model, cf. [5], for predicting inhomogeneous plastic deformation in glassy polymers. Thereafter, Section 2.1 describes the proposed fatigue model and its numerical treatment in detail. Modeling of fatigue behavior per se is based on an appealing model introduced in [33], which model is formulated in continuum mechanics framework by using evolution equations that make the definition of damage changes per cycle redundant, i.e. cycle-counting techniques do not need to be applied. The approach is calibrated to data taken from both cold drawing experiments and isothermal fatigue tests on dumbbell shaped PC-specimens. Sections 3 and 4 are dedicated to the evaluation of the proposed approach through tangible examples where the model results are compared with experimental observations.

2   The model

The governing constitutive model employed here has been introduced in a previous study [13]. The model is a three dimensional extension of the BPA model, [5]. The extended model is aimed at long-term investigations of the mechanical behavior of amorphous glassy polymers under repeated loadings. Since amorphous polymers show a notable time dependent behavior under loading cycles, i.e. the polymer chains need a relaxation time to attain their equilibrium state after deformation, both viscoelastic and viscoplastic ingredients need to be included in the model. A more detailed account of the applied constitutive model and its numerical treatment is given in [13] and [14].

2.1   Fatigue model

When dealing with fatigue under variable complex loadings, a suitable damage rule constitutes an integral part of the analysis. The stress approach, which has been reported to be suitable for the modeling of mechanically dominated, relatively brittle and high-cycle fatigue, is considered as a basis of the proposed fatigue model. Majority of the those approaches represents fatigue-limit criteria in which the fatigue limits are described under infinite number of identical cycles, [34], [26]. For finite life predictions, however, those models are equipped with cumulative damage theories, which describe the damage increase per cycle and thus require that the loading consists of well-defined cycles, [29], [34], [26]. To define equivalent, representative cycles for load histories, cycle-counting methods need to be applied, cf. [9]. However, it is often challenging to extract equivalent cycles from complex load spectrum, which characteristic makes the cycle-counting approaches difficult for demanding applications in practice. Another way is to formulate the fatigue damage model within continuum damage mechanics (CDM) framework without need to measure damage changes per loading cycles, [32], [35], [19], [22]. However, those approaches as such are not suitable for modeling fatigue in amorphous polymers.

An appealing model suitable to describe a long-term fatigue failure behavior was proposed by Ottosen et al. [33]. According to this model, uniaxial and multiaxial stress states are treated in a unified manner for arbitrary loading histories, thus avoiding cycle-counting methods. Exploiting this evolution equation based fatigue modeling concept, a model for predicting the fatigue life of amorphous glassy polymers is proposed. The model uses only few macroscopical quantities and a single parameter set, which property makes the model simple and suitable for applications in practice.
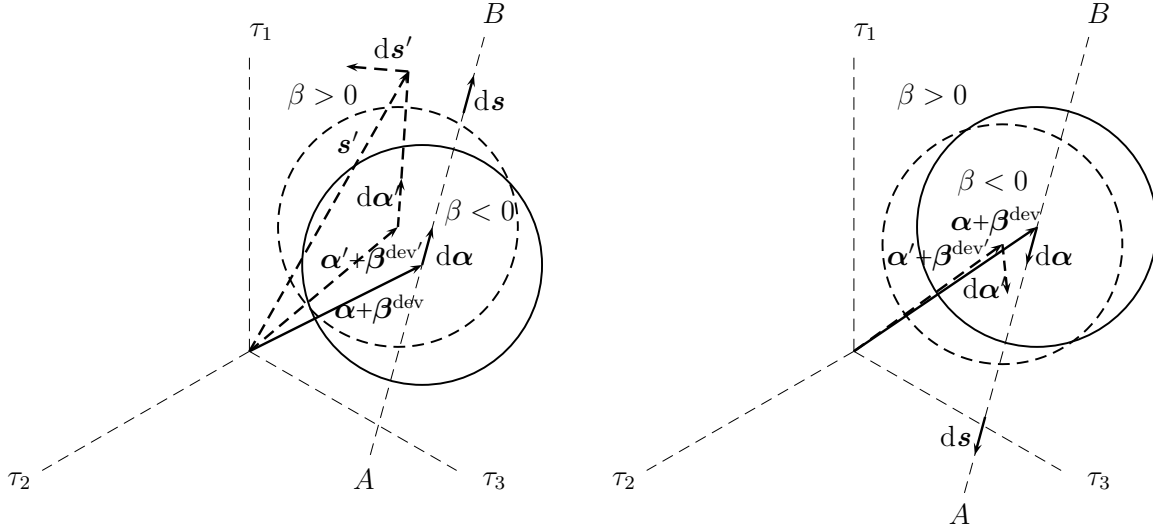
Figure 1: Alternating uniaxial stress state. The endurance surface will track the stress point and then moves between the states A and B (generally not fixed). Peripheries of the endurance surfaces in the initial and final state are highlighted by the dashed and solid line, respectively.

Due to crazing and the existence of voids around the chain molecules and inclusions, the microscopic yield of amorphous glassy polymers may depend on hydrostatic pressure, [38], [8]. In that context, any flow rule where the volumetric deformation is suppressed is not solely a sufficient rule for modeling fatigue. In the proposed model, the plastic deformation and fatigue damage are defined by the two evolution equations, respectively. The evolution equation for the plastic deformation does not include volumetric effects while for the fatigue damage it does. The model for fatigue is based on the concept of a moving endurance surface in the stress space and on an evolving damage variable, [33]. For many amorphous glassy polymers such an endurance surface can be identified, i.e. the cyclic lifetime increases with a decreasing accumulation of applied stress suggesting well-defined plateau when ultimate failure can finally reached at finite numbers of cycles just above the endurance limit. Wöhler curves are commonly used to illustrate those characteristics and identify polymers' endurance limits.

The endurance surface is considered as a function of the stress history and it can move in the stress space. In contrast to the plasticity theories for metals where the endurance surface may lie inside the yield surface, the fatigue damage development in amorphous glassy polymers is always induced by the propagation of plastic deformation. Also, since the polymer chains start align with the loading direction already at relatively low stresses and plastic strains, polymer materials show an anisotropic response which is in the model described by the backstress, $\boldsymbol{\beta}$. Due to that reasoning, the backstress is included to the endurance function. The expression of the backstress is defined adopting the BPA model, [13]. To include also volumetric damage effects, use is made of the endurance surface as

$$\beta = \frac{1}{S_0}(\bar{\tau} + aI_1 - S_0) = 0 \tag{1}$$

where the effective stress $\bar{\tau}$ is defined in terms of the second invariant of the reduced deviatoric stress $\boldsymbol{s} - \boldsymbol{\beta}^{\mathrm{dev}} - \boldsymbol{\alpha}$ as

$$\bar{\tau} = \sqrt{3J_2(\boldsymbol{s} - \boldsymbol{\beta}^{\mathrm{dev}} - \boldsymbol{\alpha})} = \sqrt{\tfrac{3}{2}(\boldsymbol{s} - \boldsymbol{\beta}^{\mathrm{dev}} - \boldsymbol{\alpha}) : (\boldsymbol{s} - \boldsymbol{\beta}^{\mathrm{dev}} - \boldsymbol{\alpha})}. \tag{2}$$
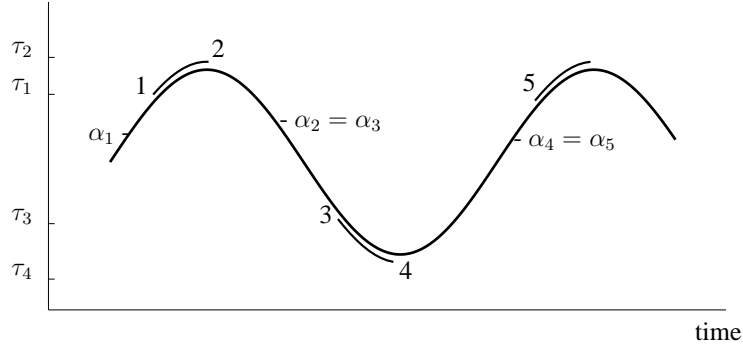
Figure 2: Alternating uniaxial loading. The damage development and movement of the endurance surface during cycling is indicated by a double curve.

In the equation (2), $s := \tau^{\mathrm{dev}}$ is the deviatoric part of the Kirchhoff stress, τ, of which the first stress invariant is given by $I_1 = \mathrm{tr}\,\tau$, cf. [13]. α is a fatigue backstress defined subsequently. The invariant I_1 reflects the effect of mean stress, i.e. the hydrostatic tension enhances the fatigue development while fatigue is suppressed under hydrostatic compression. The parameter a in (1) is considered as positive and dimensionless which in uniaxial cyclic loadings determines the slope of the Haigh-diagram. The last parameter S_0 is the endurance limit for zero mean stress. Shape of the endurance surface in the deviatoric plane is circular as illustrated in Fig. 1.

When low-cycle fatigue is studied, the impact of the backstress β on fatigue is significant since its magnitude in relation to the stress is large. Then, the backstress is considered as a driving force for fatigue damage through the localized plastic deformation in the material. When reducing stresses and strains, the effect of the backstress decreases and another backstress quantity α dominates the fatigue damage development. In high-cycle regime, the presence of α in the fatigue model is mandatory in order to govern fatigue of virtually elastic responses (cf. e.g. steels).

The center point of the endurance surface is defined by the $\alpha + \beta^{\mathrm{dev}}$ tensor as depicted in Fig. 1. Once an alternating loading is applied, the endurance surface will track the current stress point since the movement of α always is in the direction of $s - \beta^{\mathrm{dev}} - \alpha$. It is the $\alpha + \beta^{\mathrm{dev}}$ tensor which memorizes the load history and results in the movement of the endurance surface in the stress space. The evolution of α is governed by a hardening rule similar to the Ziegler's kinematic hardening rule in plasticity theory, i.e.

$$\dot{\alpha} = C(s - \beta^{\mathrm{dev}} - \alpha)\dot{\beta}, \tag{3}$$

where C is a non-dimensional material parameter. The volumetric damage effects are included into (3) through the endurance surface (1). Since α is considered an overall driving force for fatigue damage, it evolves only if the current stress state is outside the endurance surface, i.e.

$$\beta \geq 0, \quad \dot{\beta} \geq 0 \quad \Rightarrow \quad \dot{D} \geq 0, \quad \dot{\alpha} \neq \mathbf{0}. \tag{4}$$

Referring to Fig. 2 for an alternating uniaxial loading, the concept is further demonstrated, see also [33] for a more detailed account. During loading from the state 1 to 2, the stress state lies outside the endurance surface and damage evolves, i.e. $\beta > 0$ and $\dot{\beta} > 0$. Between the states 2 and 3, the stress path has crossed the endurance surface and the stress state enters the space within the endurance surface. Then, $\beta > 0$ and $\dot{\beta} < 0$ when damage and the backstress do not evolve, i.e. $\dot{D} = 0$ and $\dot{\alpha} = 0$ until the stress path crosses again the current endurance surface at the state 3. It then follows that $\alpha_3 = \alpha_2$. From the state 3 to 4, damage again

5

evolves. In accordance with the stress path between the states 2 and 3, the damage development is inhibited until the state 5 is reached, i.e. $\alpha_5 = \alpha_4$.

Damage evolution

Despite possible strain hardening and subsequent directional damage fields especially in large deformations, the fatigue behavior is described by a scalar valued quantity so as to keep the model simple. Assuming damage increases nonlinearly with the distance from the endurance surface, an exponential form

$$\dot{D} = K \exp(f(\beta; L_1, L_2, \vartheta))\dot{\beta}, \tag{5}$$

with the values $0 \leq D \leq 1$, is chosen for the damage evolution law. In (5), K, L_1, L_2, and ϑ are material parameters.

Many amorphous glassy polymers (such as PC) show only a moderate increase of the applied stress as the cyclic lifetime reduces. To capture such a behavior, a function f having two linear asymptotes for positive β is defined, i.e.

$$f(\beta; L_1, L_2, \vartheta) = L_1\beta - L_2 \left[\beta + \frac{L_2}{\vartheta} \left(\exp(-\vartheta\beta/L_2) - 1 \right) \right], \tag{6}$$

which has the asymptote $L_1\beta$ when $\beta \to 0$ (HCF-regime) and $(L_1 - L_2)\beta$ when β is large (LCF-regime). The curvature ϑ determines how rapidly the second asymptote is reached.

Since damage never decreases, it appears from (5) that $\dot{\beta} \geq 0$, i.e. damage rate increases with the distance from the endurance surface. Furthermore, damage develops only if stress states lie outside the endurance surface, i.e. $\beta > 0$ and the condition (4) is fulfilled.

3 Calibration of the model

The governing constitutive model was first calibrated to data obtained from cold drawing experiments on dumbbell shaped PC-specimens. Fatigue was omitted at this phase. A more detailed account for the test program involving repeated loading cycles is found from [13]. The calibrated parameters are listed in Table 1.

The parameters for modeling fatigue were determined from in situ measurements taken from [17] and [18]. Material which has been employed in the tensile fatigue test is a quenched PC (Lexan® 101R and 161R) and a specimen geometry used for fatigue studies includes a common dumbbell-shaped, injection molded tensile specimen (ASTM D638-IV), cf. [1], [2], and [10]. Isothermal test conditions for mechanically induced fatigue involve uniaxial stress submitted to load control at the room temperature of 23°C.

Table 1: Constitutive model parameters for PC. The calibration of the model is based on the the cold drawing experiments on a dumbbell shaped test specimens. The remaining viscoelastic constitutive parameters are $E = 2550$ MPa, $E_1 = 1295$ MPa, $\eta = 1.5 \cdot 10^5$ MPas, and $\nu = 0.37$.

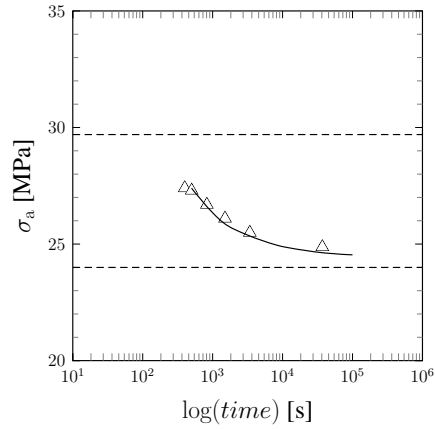| Parameter	s_0	s_{ss}	h_1	$\dot{\gamma}_0$	A	C^{R}	N	α
Unit	MPa	MPa	MPa	s^{-1}	$\mathrm{MPa}^{-1}K$	MPa		
Value	96	76	720	$5.6 \cdot 10^{15}$	240	14	2.2	0.08

Figure 3: Fatigue strengths ($\sigma_{\mathrm{m}} = \sigma_{\mathrm{a}} + 2.2$ MPa) for PC employed (left). The solid line denotes the model result, and the marker $\triangle$ refers to data points taken from [18]. The upper and lower horizontal dashed line refer to the static tensile yield strength and an estimated endurance limit, respectively.

According to the test, the maximum stress level of a sine wave varies, while the minimum stress level is kept at 2.2 MPa. The frequency applied is 2 Hz, [18].

First, the slope a of the Haigh-diagram was extracted from data given in [17] (Fig. 11a). The fatigue limit S_0 for zero mean stress and the remaining parameters C, K, L_1, L_2, and ϑ were calibrated to data shown in Fig. 3. The calibrated parameters are given in Table 2 and the model response is depicted in Fig. 3. The results indicate that the cyclic lifetime smoothly decreases with increasing accumulation of applied stress. Reducing the stress level, a transition in the failure mode occurs from ductile to brittle, i.e. ultimate failure can finally reached at finite numbers of cycles right above an expected endurance limit.

4 Results and discussion

4.1 Uniaxial stress state

Based on the calibrated parameters in Tables 1 and 2, the capability of the model to predict fatigue phenomena is discussed. The development of the movement of the endurance surface under a sinusoidal cyclic tension is demonstrated in Fig. 4. Right once the periodic loading is applied, the endurance surface reaches its periodic state similar to demonstrated in Fig. 1. During cycling, damage develops as the stress state is outside the endurance domain and moves away from it, i.e damage always increases when the endurance limit in Fig. 4 shows an increase and the stress is greater than the endurance limit. This situation was already illustrated in Fig. 2. Since the endurance limit in relation to the maximum stress is now low, damage increases rapidly leading to a short fatigue life as it is depicted in Fig. 5.

Table 2: Material parameters of the fatigue model for PC. The calibration is based on the cyclic tension experiments on a uniaxial tensile bar given in [17] and [18].

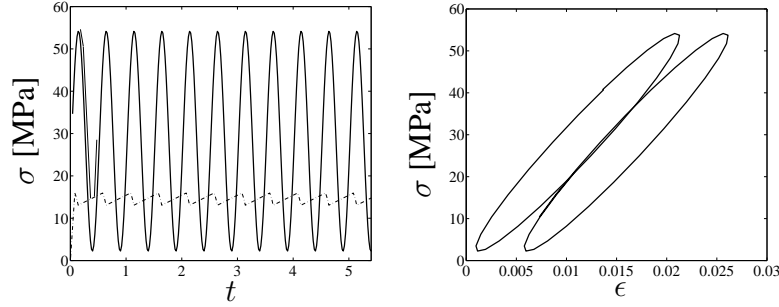| Parameter	S_0	a	C	$K \cdot 10^{-3}$	L_1	L_2	ϑ
Unit	MPa						
Value	28.0	0.95	0.05	5.8	18.0	4.0	2.0

Figure 4: The cyclic true stress (solid thick line) and the periodic movement of the endurance limit (dash-and-dot line) during first few stress cycles (left). The damage development during the first cycle is indicated by the double curve. Model predictions for the second and last (prior to failure) hysteresis loops (right).
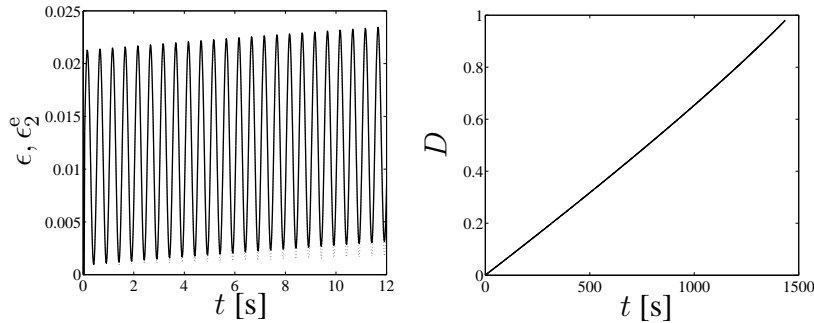

Figure 5: The periodic development of the true strain (solid line) and its viscoelastic component (dashed line) at the beginning of cycling tension. The corresponding cyclic stress is shown in Fig. 4 (left). Development of damage variable according to (5) (right).

Hysteresis loops of PC demonstrated in Fig. 4 show a constant area indicating a non-substantial energy-dissipation, i.e. hysteresis loops do not show a progressive increase in compliance and irreversible work during evolving fatigue, cf. [23], [18]. The result is a consequence of both neglected temperature effects and physical aging which is a relevant assumption under the applied low frequency loading. Fig. 5 further shows a periodically increasing development of both the true strain and its viscoelastic component at the beginning of loading. A small difference between the strains results from constantly increasing plastic strain. The growth of viscoelastic and plastic strains during the cyclic loading lead finally to a notable elongation composed of creep and plastic stretching. Considering a tensile test specimen, the elongation causes neck propagation followed by a brittle rupture as shown in [18].

Almost fully reversed uniaxial loading case (a low negative mean stress) was also studied, and the stress response as well as the corresponding hysteresis loops are shown in Fig. 6. In this situation, a reduction in the true strain is observed which feature is due to an accumulation of the viscoelastic and plastic strains. The development of the plastic strain shown in Fig. 7 refers to ratchetting, i.e. constantly accumulated plastic strain develops without bound as the cyclic loading continues, cf. [6], [21], [25]. Albeit not shown, similar phenomenon is observed in the load controlled cyclic tension, cf. Fig. 5 (left). Comparison between the first few loops and the loops prior to final failure (inset plot on the right) reveals that the area of the loops significantly increases during loading. Despite an accelerated propagation depicted in the inset plot (left),
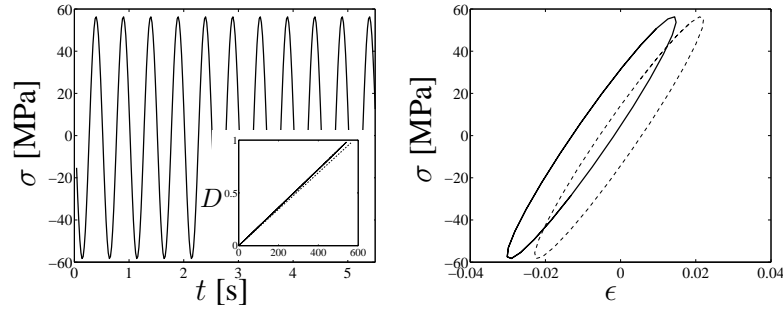
8

Figure 6: The cyclic true stress at the beginning of cycling as the frequency is 2 Hz and the maximum and minimum stresses are 56.4 MPa and -58.4 MPa, respectively (left). The inset plot shows damage increase without phase shift (solid line) and with phase shift $180°$ (dashed line). Model predictions for the second and last (prior to failure) hysteresis loops are highlighted by the dashed and solid line, respectively (right).

the final value prior to fatigue failure is still relatively low.
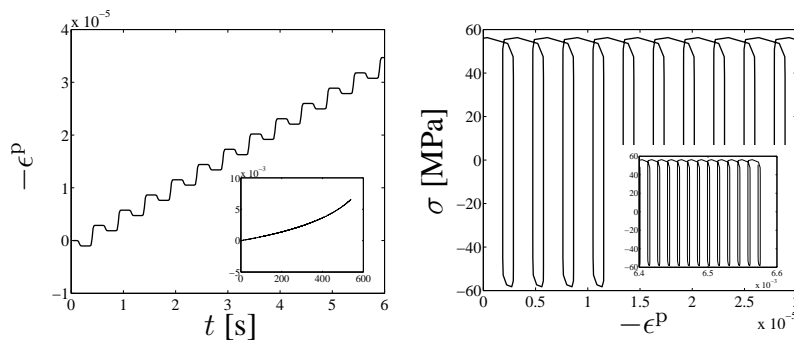

Figure 7: Periodic development of the plastic strain at the beginning of a cyclic loading (left). The inset plot shows an increase of the plastic strain up to the final failure. Stress vs plastic strain response at the beginning of loading and prior to failure (right).

Fatigue of a dumbbell shaped PC-specimen

Due to the localization of the plastic deformation, damage grows unevenly in the material leading to a reduced fatigue life somewhere in the material. Thus, it is of interest to investigate the fatigue damage development of the entire test specimen by using a finite-element method. The specimen's geometry, loading conditions as well as details for the applied finite element mesh are found from [13].

Fig 8 shows that the damage development progresses most intensively in the gauge section of the specimen. This characteristic is because of an increasing localized plastic deformation and necking during drawing, cf. [13]. The predicted progress of fatigue damage is in line with experimentally observed macroscopic failure behavior of PC (at the same load) which shows a stable neck growth followed by a rapid rupture, cf. e.g. [18]. It is largely acknowledged that crazing is the governing micro-mechanism that triggers the fatigue damage at the sites following closely the localization of the plastic deformation in the amorphous glassy matrix, [11], [15], [7], [23].
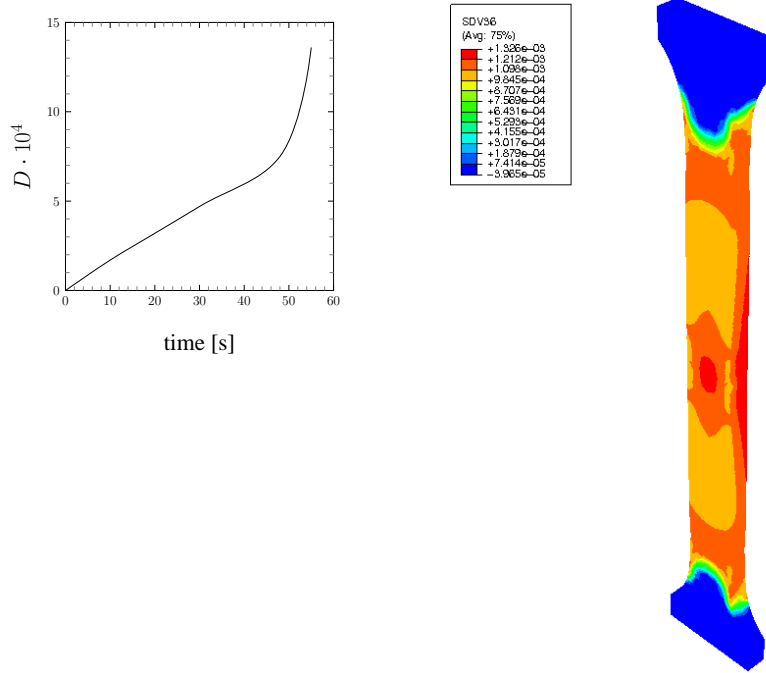
Figure 8: Damage development in a dumbbell shaped test specimen right after 100 cycles (right). The plot on the left shows the damage development in the middle of the specimen. A stable damage growth initiates after 50 seconds. The minimum and maximum pressure employed at the bottom edge are 1.1 MPa and 28.1 MPa, respectively. The corresponding average stress state in the gauge section is twofold.

A glance at Fig. 3 reveals that the fatigue life of the specimen under this loading should remain under 400 cycles. Considering the result in Fig. 8, solely the calculation of the solution for one hundred cycles took several hours. For this reason, when long term predictions are investigated, the fatigue life (e.g. for steels) is traditionally evaluated by using the location of most evolving fatigue observed at the beginning of the loading. However, due to a neck initiation, the damage response shows a nonlinear accumulation which feature makes a reliable prediction of the forthcoming damage and following fatigue life somewhat challenging. The evaluation of the fatigue life is computationally expensive since the analyzes must continue once a stable neck and damage growth are reached.

Conclusions

The celebrated 8-chain BPA (Boyce-Parks-Argon) model was extended to cover fatigue damage behavior intrinsic to polymers of amorphous classes. When dealing with fatigue under variable complex loadings, a suitable damage rule constitutes an integral part of the analysis. A fatigue model proposed here is an extension of the appealing model given by Ottosen et al. [33], which model is formulated in continuum mechanics framework by using evolution equations that make the definition of damage changes per cycle redundant, i.e. cycle-counting techniques do not need to be applied. The model was calibrated to data taken from an accelerated uniaxial fatigue testing of PC with a high mean stress.

To investigate the propagation of fatigue damage under multiaxial cyclic loading conditions, the proposed approach was implemented in a finite element program. Finite element studies of a dumbbell-shaped test specimen were performed for analyzing the effect of plastic instabilities on fatigue damage. The proposed approach predicted the progress of fatigue damage

which was shown to be in line with experimentally observed macroscopic failure behavior of PC. The results indicated that localized yield-like deformation provides fatigue crack initiation sites which control the fatigue propagation and eventually the entire fatigue life of amorphous glassy polymers. When based solely on previous, short-term damage histories, the prediction of forthcoming damage development and the following fatigue life was shown to be challenging due to the plastic instabilities. The evaluation of the fatigue life was reliable only once a stable neck and damage growth were reached.

References

[1] ASTM, 1985. ASTM D638, Standard for Uniaxial Tensile Testing. American Society for Testing and Materials, Philadelphia, Pa.

[2] ASTM, 1985. ASTM D671, Standard for Metric Practice. American Society for Testing and Materials, Philadelphia, Pa.

[3] Baltenneck, F., Trotignon, J.-P., Verdu, J., 1997. Kinetics of fatigue failure of polystyrene. Polym. Engngn. Sci. 37, 1740–47.

[4] Beardmore, P., Rabinowitz, S., 1975. Fatigue deformation in polymers. In: Plastic Deformation of Materials: Treatise on Materials Science and Technology; Arsenault, R. J., Ed. Academic Press: New York.

[5] Boyce, M. C., Parks, D. M., Argon, A. S., 1988. Large inelastic deformation of glassy polymers, Part I: Rate-dependent constitutive model. Mechanics of Materials 7, 15–33.

[6] Chaboche, J. L., 1991. On some modifications of kinematic hardening to improve the description of ratchetting effects. Int. J. Plasticity 7, 661–678.

[7] Drozdov, A. D., 2000. Nonlinear viscoelasticity and fatigue of glassy polymer. Mech. Res. Comm 27, 281–286.

[8] Estevez, R., Tijssens, M. G. A., Van der Giessen, E., 2000. Modeling of the competition between shear yielding and crazing in glassy polymers. J. Mech. Phys. Solids 48, 2585–2617.

[9] Fatemi, A., Yang, L., 1998. Cumulative fatigue damage and life prediction theories: a survey of the state of the art for homogeneous materials. International Journal of Fatigue 20, 9–34.

[10] Foster, A. M., May 2015. Materials testing standards for additive manufacturing of polymer materials: State of the art and standards applicability. Tech. rep., Materials and Structural Systems Division Engineering Laboratory, NISTIR 8059.

[11] Henkee, C. S., Kramer, E. J., 1984. Crazing and shear deformation in crosslinked polystyrene. Polymer 22, 721–737.

[12] Hertzberg, R. W., Manson, J. A., 1980. Fatigue of Engineering Plastics. Academic Press, New York.

[13] Holopainen, S., 2013. Modeling of the mechanical behavior of amorphous glassy polymers under variable loadings and comparison with state-of-the-art model predictions. Mechanics of Materials 66, 35–58.

[14] Holopainen, S., 2014. Influence of damage on inhomogeneous deformation behavior of amorphous glassy polymers. Modeling and algorithmic implementation in a finite element setting. Engng. Fract. Mech. 117, 28–50.

[15] Hristov, H. A., Yee, A. F., Gidley, D. W., 1994. Fatigue craze initiation in polycarbonate: study by transmission electron microscopy. Polymer 35, 3604–11.

[16] James, M. N., Christopher, C. J., Y. Lu, E. A. P., 2012. Fatigue crack growth and craze-induced crack tip shielding in polycarbonate. Polymer 53, 1558–70.

[17] Janssen, R. P. M., Govaert, L. E., Meijer, H. E. H., 2008. An analytical method to predict fatigue life of thermoplastics in uniaxial loading: Sensitivity to wave type, frequency, and stress amplitude. Macromolecules 41, 2531–40.

[18] Janssen, R. P. M., Kanter, D. K., Govaert, L. E., Meijer, H. E. H., 2008. Fatigue life predictions for glassy polymers: A constitutive approach. Macromolecules 41, 2520–30.

[19] Kawai, M., 2004. A phenomenological model for off-axis fatigue behavior of unidirectional polymer matrix composites under different stress ratios. Composites Part A: Applied Science and Manufacturing 35, 955–963.

[20] Kung, E., Mercer, C., Allameh, S., Popoola, O., Soboyejo, W., 2001. An investigation of fracture and fatigue in a metal/polymer composite. Metall Mater Trans A 32, 1997–2010.

[21] Lemaitre, J., Chaboche, J. L., 1994. Mechanics of Solid Materials. Cambridge University Press, Cambridge.

[22] Lemaitre, J., Desmorat, R., 2005. Engineering Damage Mechanics. Ductile, Creep, Fatigue and Brittle Failures. Springer-Verlag, Berlin.

[23] Lesser, A. J., 2002. Fatigue behavior of polymers. In: Encyclopedia of Polymer Science and Technology 6, 197–251.

[24] Lewis, P. R., 2009. Environmental stress cracking of polycarbonate catheter connectors. Engineering Failure Analysis 16, 1816–24.

[25] Liu, W., Gao, Z., Yue, Z., 2008. Steady ratcheting strains accumulation in varying temperature fatigue tests of PMMA. Materials Science and Engineering A 492, 102–109.

[26] Liu, Y., Mahadevan, S., 2007. A unified multiaxial fatigue damage model for isotropic and unisotropic materials. International Journal of Fatigue 29, 347–359.

[27] Lu, H., Kim, G., 2007. Characteristics of accelerated lifetime behavior of polycarbonate under athermal and high loading frequency conditions. Polymer Testing 26, 839–45.

[28] Luu, D., Maitournam, M., Nguyen, Q., April 2014. Formulation of gradient multiaxial fatigue criteria. International Journal of Fatigue 61, 170–183.

[29] Matake, T., 1977. An explanation on fatigue limit under combined stress. Bulletin of the Japan Society of Mechanical Engineers 20, 257–263.

[30] Maxwell, A. S., Broughton, W. R., Dean, G., Sims, G. D., 2005. Review of accelerated ageing methods and lifetime prediction techniques for polymeric materials. Tech. rep., National Physical Laboratory Hampton Road, Teddington, Middlesex, TW11 0LW.

[31] Melick, H. G. H. V., 2003. Deformation and failure of polymer glasses. Doctoral thesis. University Press Facilities, Eindhoven.

[32] Okui, Y., Horii, H., Akiyama, N., 1993. A continuum theory for solids containing microdefects. Int. J. Engng. Sci. 31, 735–749.

[33] Ottosen, N., Stenström, R., Ristinmaa, M., June 2008. Continuum approach to high-cycle fatigue modeling. International Journal of Fatigue 30 (6), 996–1006.

[34] Papadopoulos, I. V., 2001. Long life fatigue under multiaxial loading. International Journal of Fatigue 23 (10), 839 – 849.

[35] Peerlings, R., Brekelmans, W., de Borst, R., Geers, M., 2000. Gradient-enhanced damage modelling of high-cycle fatigue. International Journal for Numerical Methods in Engineering 49 (12), 1547–1569.

[36] Ritchie, R. O., 1999. Mechanisms of fatigue-crack propagation in ductile and brittle solids. Int. J. Fracture 100, 55–83.

[37] Shah, Q. H., Abakr, Y. A., 2008. Effect of distance from the support on the penetration mechanism of clamped circular polycarbonate armor plates. Journal of Impact Engineering 25, 1244–50.

[38] Steenbrink, A. C., Van der Giessen, E., 1998. Studies on the growth of voids in amorphous glassy polymers. Journal of Material Sciences 33, 3163–3175.

[39] Takemori, M. T., Kambour, R. P., Matsumoto, D. S., 1983. On a search for epsilon crack tip plastic zones in the fatigue of amorphous polymer. Polym. Comm 24, 297–299.

[40] Takemori, M. T., Matsumoto, D. S., 1985. Shear and craze development in the fatigue of ductile amorphous polymers. Journal of Material Sciences 20, 873–880.

[41] Tauchert, T. R., 1967. Int. J. Engng. Sci., 353–365.